

Table 1 Experimental conditions and calculated  $T_0$  from present work and Refs. 1-3

	Papanikas' nozzle, argon, $p_0 = 0.408$ atm, $\dot{m} = 0.695$ g/sec, $T_0$ , K	Bachour's nozzle, nitrogen, $p_0 = 1$ atm, $\dot{m} = 0.9$ g/sec, $T_0$ , K	Carden's nozzle, nitrogen, $p_0 = 1.21$ atm, $\dot{m} = 0.4536$ g/sec, $T_0$ , K
One-dimensional isentropic frozen up to throat	3234	...	3373
One-dimensional isentropic equilibrium up to throat	...	2800	2875
Slender channel frozen	3828	...	3598
Slender channel, vibrational nonequilibrium, fully catalytic wall	...	3195	3516
Slender channel, vibrational nonequilibrium, $\alpha_v \ll 1$	...	3179	3486

cooling was 225.5 J/sec, nearly 16.5% of the initial power input. The value of  $P$  at the throat was 1135 J/sec, and the average  $T_0$  at the throat was 3140 K, which was quite close to the  $T_0$  calculated from the inviscid flow model.

Flowfields at the nozzle exit computed by the present method have been presented in Refs. 6 and 7. Generally, they compare well with available experimental results. We may conclude by noting that slender channel equations provide a realistic alternative way to calculate average stagnation chamber temperature in high-enthalpy, low Reynolds number frozen or vibrational nonequilibrium nozzle flow from experimentally measurable data of  $p_0$ ,  $\dot{m}$ , and nozzle wall temperature. The present method is more time-consuming than simple one-dimensional inviscid approximation but should be recommended for flow with high stagnation temperature where the nozzle wall is subjected to intense cooling. Our calculations show that for such flows the  $T_0$  calculated by the inviscid flow model may lead to error up to 20% for argon and 10% for nitrogen. It also should be noted that zero wall catalyticity for vibrational energy in a cooled-wall nozzle compares better with experiment than fully catalytic wall. Further modifications of the present method to include dissociation of the flow medium are underway.

### References

- <sup>1</sup>Papanikas, D.G., "Investigations of Axisymmetric Hypersonic Free Jets in High Total Enthalpy Wind Tunnels," ESRO TT-150, March 1975, European Space Research Organization.
- <sup>2</sup>Bachour, F. and Erdtel, D., "Experimental Investigations of Hypersonic Low-Density Flows behind Water-cooled and Liquid-Nitrogen-Cooled Nozzles in DFVLR Wing Tunnel PK-1," ESRO TT-129, Feb. 1975, European Space Research Organization.
- <sup>3</sup>Carden, W. H., "Local Heat-Transfer Coefficients in High-Speed Laminar Flow," *AIAA Journal*, Vol. 3, Dec. 1965, pp. 2183-2189.
- <sup>4</sup>Williams, J.C., III, "Viscous Compressible and Incompressible Flow in Slender Channels," *AIAA Journal*, Vol. 1, Jan. 1963, pp. 186-195.
- <sup>5</sup>Rae, W. J., "Final Report on a Study of Low-Density Nozzle Flows, with Application to Micro Thrust Rockets," CAL AI-2590-A-1, Dec. 1969, Cornell Aeronautical Laboratory, Inc., Buffalo, N.Y.
- <sup>6</sup>Mitra, N.K. and Fiebig, M., "Low Reynolds Number Hypersonic Nozzle Flows," *Zeitschrift für Flugwissenschaften*, Vol. 2, Feb. 1975, pp. 39-45.
- <sup>7</sup>Mitra, N.K. and Fiebig, M., "Low Reynolds Number Vibrational Nonequilibrium Flow in Laval Nozzle," *Proceedings of the Ninth International Symposium on Rarefield Gas Dynamics*, July 1974, pp. B.21-1 to B.21-12.
- <sup>8</sup>Lunkin, Yu. P., "Vibrational Dissociation Relaxation in a Multicomponent Mixture of Viscous Heat-Conducting Gases," *IUTAM Symposium on Irreversible Aspects of Continuum Mechanics*

and Transfer of Physical Characteristics in Moving Fluids, 1966, Vienna, pp. 228-236.

<sup>9</sup>Mitra, N.K. and Fiebig, M., "Flow Field Computation through Sonic Singularity in Viscous Frozen and Nonequilibrium Nozzle Flow," *GAMM Conference on Numerical Methods in Fluid Mechanics*, Oct. 1975, Cologne, West Germany.

## Temperature Measurements in Rail Electrode Cross-Flow Arcs

D.M. Benenson\* and J.J. Nowobilski†  
State University of New York at Buffalo,  
Buffalo, N.Y.

TEMPERATURE diagnostics in cross-flow arcs have been previously reported for pin electrode configurations operated with an applied transverse magnetic field.<sup>1,2</sup> and in the absence of such a field,<sup>3</sup> i.e., with forced convection alone. The rail electrode arrangement frequently is found in circuit breaker applications; here, interactions of the magnetic field with the arc column play an important role. As an initial step in the study of the time-varying, nonstationary cross-flow arc, the experiments reported herein were carried out upon a steady-state rail electrode configuration, which was maintained stationary (i.e., "balanced" with respect to flow and magnetic effects) through application of a magnetic field transverse to the mainstream flow.

Tests were conducted with a 100 A argon arc operated at about 840 Torr. The mainstream flow velocity ranged from about 3.7 to about 7.3 m/sec; the maximum value of the applied magnetic field was 68 G. Electrode spacing was 1.27 cm. Experiments were conducted in an open-circuit test facility,<sup>1-3</sup> the test section of which was 43 cm long with cross-section

Received Oct. 20, 1975. This research was supported by U.S. Office of Scientific Research Grant 70-1928 and by National Science Foundation Grant ENG74-15272.

Index categories: Plasma Dynamics and MHD; Electric Power Generation Research; Electric and Advanced Space Propulsion.

\*Professor, Faculty of Engineering and Applied Sciences.

†Research Assistant, Faculty of Engineering and Applied Sciences; presently Assistant Staff Engineer, Linde Division of Union Carbide, Tonawanda, N.Y.

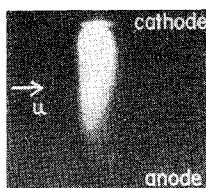


Fig. 1 Straight arc:  $I = 100$  A,  $g = 1.27$  cm,  $u = 3.65$  m/sec,  $B = 10$  G.

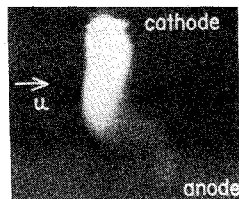


Fig. 2 S-shaped arc:  $I = 100$  A,  $g = 1.27$  cm,  $u = 7.31$  m/sec,  $B = 68$  G.

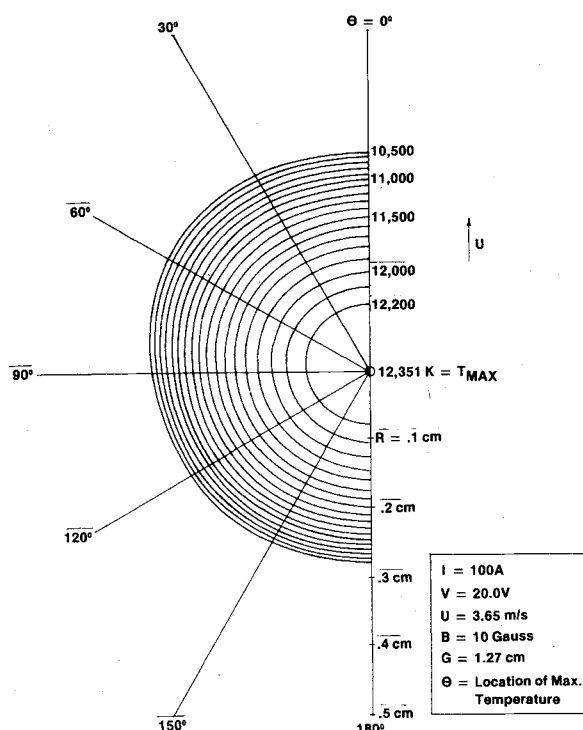


Fig. 3 Isotherm distributions, straight arc:  $I = 100$  A,  $g = 1.27$  cm,  $u = 3.65$  m/sec,  $B = 10$  G; 0.64 cm from cathode.

4.5 × 4.5 cm. A viewing window, 33 cm long, permitted observation of the arc over a wide range of azimuthal angles ( $\theta$ ). The rails (tantalum cathode, copper anode) were 17.2 cm long, including a 1.9-cm fairing at the upstream ends. In cross-section, the rails contained a 75° wedge to which the arc was attached.

Temperature distributions within the column were obtained by using the optical techniques previously developed<sup>1-3</sup> for configurations having noncircular cross sections. This arrangement allowed the radiation from the arc to be observed and recorded (photographically) simultaneously at 12 azimuthal locations. Inversion of the resulting integrated intensity distributions to the distribution of local emission coefficients was obtained using the procedures of Ref. 4. Temperatures were determined from a Kramers-Untsold equation for the argon continuum.

The experimental results showed that, depending upon the operating conditions, three column configurations could be obtained: straight arc (i.e., column oriented perpendicular to the electrodes and to the mainstream flow), Fig. 1; slanted arc [typically with the anode attachment downstream of the cathode root; slant angles (with respect to the normal to the electrodes) were about 10°]; and S-shaped arc, in which a

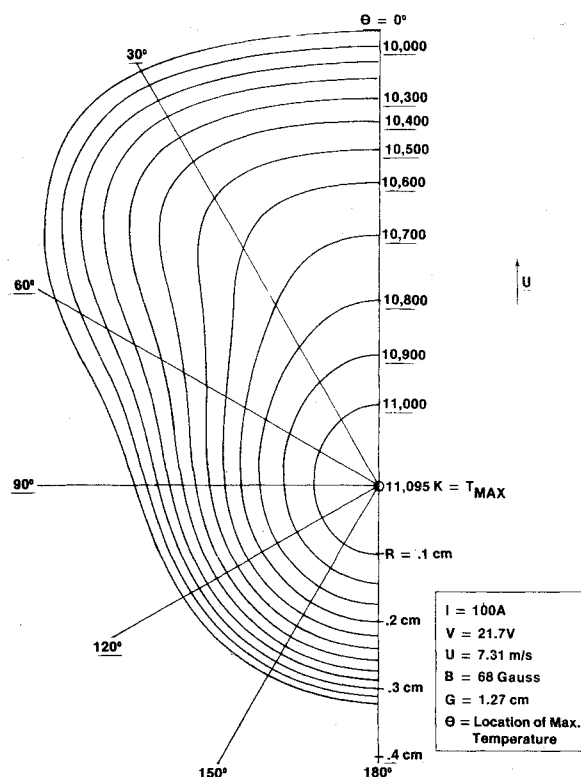


Fig. 4 Isotherm distributions, S-shaped arc:  $I = 100$  A,  $g = 1.27$  cm,  $u = 7.31$  m/sec,  $B = 68$  G; 0.89 cm from cathode.

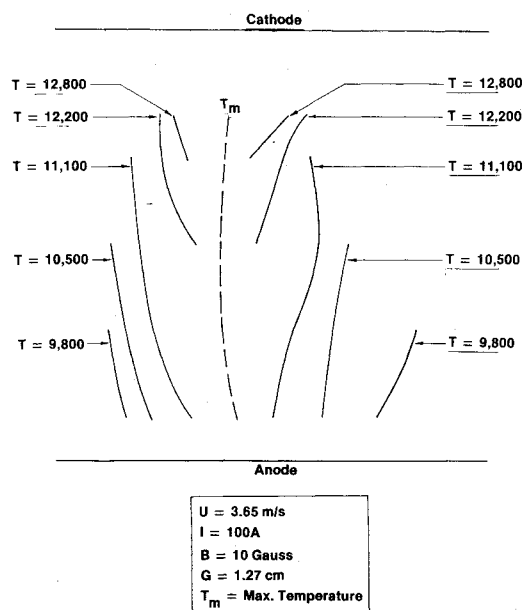


Fig. 5 Arc profile, straight arc:  $I = 100$  A,  $g = 1.27$  cm,  $u = 3.65$  m/sec,  $B = 10$  G.

significant portion of the column was parallel to the flow direction, Fig. 2. In all cases, the arc dimensions in the flow and transverse directions were larger at the anode than at the cathode. In this respect, it should be noted that determination of arc dimensions from photographic prints (as in Figs. 1 and 2) is an unreliable method; the corresponding negatives are an improvement. Through the methods described in Refs. 1-3, isotherm distributions (in the horizontal plane) were obtained at several locations within the column. These distributions clearly indicated the relatively large dimensions associated with the anode attachment region. Furthermore, the cathode root accommodated (or reacted to) changes in the flow or applied magnetic fields much more slowly than the anode at-

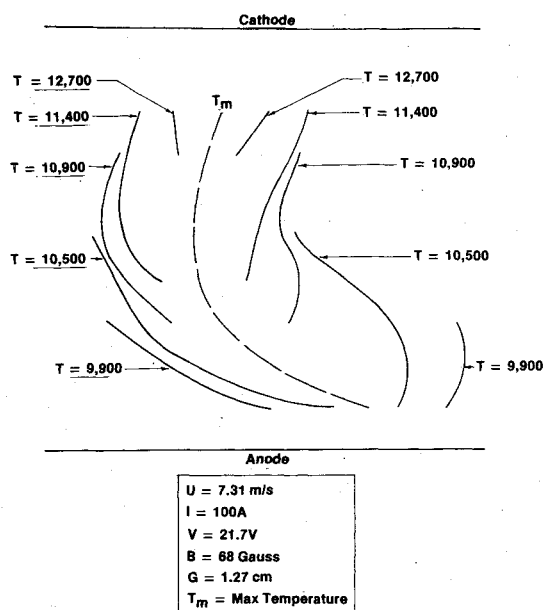


Fig. 6 Arc profile, S-shaped arc:  $I=100$  A,  $g=1.27$  cm,  $u=7.31$  m/sec,  $B=68$  G.

tachment. In previously reported experiments on balanced rail arcs, e.g., Refs. 5-7, (1) the slanted arc alone seemed to be found, (2) the cathode root was downstream of the anode attachment, and (3) the arc appeared larger in dimension near the cathode. The differences between the present results and the foregoing with respect to the size of the regions near the roots and thus, most probably, the determination of the downstream attachment, were probably due to electrode and electrode material effects. The present results were consistent with the analysis of Ref. 6 which, assuming the cathode attachment to be fixed (as essentially observed herein), predicted the relative locations of the arc roots and the overall profile of the column. For the flow-determined case therein, the anode root was predicted to be the downstream attachment; the relations describing this case were satisfied in the present experiments. Furthermore, in the limiting case of the flow-determined arc, the column was shown to contain a segment parallel to the flow, as was found in Fig. 2.

Isotherm distributions in the horizontal plane of the column and at midheight between the electrodes (0.64 cm from the cathode) are shown in Fig. 3 for the straight arc (of Fig. 1). The distributions for all column configurations were found to exhibit a mirror plane of symmetry (along the  $\theta=0^\circ$ - $180^\circ$  axis, i.e., parallel to the direction of flow). The ellipticity of a given isotherm can be characterized by the axis ratio,  $AR$ , defined as the ratio of the distance between the intercepts (of the isotherm) along the mirror plane of symmetry ( $\theta=0^\circ$ - $180^\circ$  axis) to that along the  $\theta=90^\circ$  azimuth. Values of  $AR>$  or  $<1$  suggest an emphasis of magnetic or flow effects, respectively;  $AR=1$  indicates a tendency for a circular distribution. For the case shown in Fig. 3,  $AR\sim 1.03$  for the inner and outer isotherms ( $T=11,900$  and  $10,500$  K, respectively). Over the range of velocities with the straight arc ( $\sim 3.7$ - $7.3$  m/sec), the axis ratio ranged from 0.93 to 1.04. With pin electrodes, balanced arcs (with attachments at or near the apexes of the electrodes) were found to have axis ratios in the range 1.06 to 1.18,<sup>1,2</sup> with velocities in the range  $\sim 1.8$ - $5.1$  m/sec. (In the absence of applied magnetic fields, observed axis ratios always have been less than unity<sup>3</sup> and were a strong function of velocity, decreasing to  $\sim 0.1$  at speeds near arc blowout.) Electrode effects, as related to the pin and rail configurations, probably accounted for the differences between the present results and those of Refs. 1 and 2. Analysis<sup>8</sup> of a balanced cross-flow plasma, in which the arc was assumed straight and uniform along the column (elec-

trode effects were not considered), predicted, for operating conditions  $I=30$  A,  $u=4.0$  m/sec, an axis ratio  $\sim 1.5$ .

Shown in Fig. 4 are isotherm distributions for the S-shaped arc (of Fig. 2) obtained in the portion of the column parallel to the direction of flow. The relative elongation of the column in the flow direction is apparent; here,  $AR=0.71$  at the outer ( $T=9900$  K) isotherm. Column profiles (in the mirror plane of symmetry) for the straight and S-shaped columns are shown in Figs. 5 and 6, respectively. The profiles reflect the widely different arc configurations obtained.

## References

- <sup>1</sup>Baker, A.J. and Benenson, D.M., "Effects of Forced Convection Upon the Characteristics of a Steady-State Cross-Flow Arc in the Presence of an Applied Transverse Magnetic Field," *Proceedings of the IEEE*, Vol. 59, 1971, pp. 450-457.
- <sup>2</sup>Benenson, D.M. and Baker, A.J., "Transverse Magnetic Field Effects on a Cross-Flow Arc," *AIAA Journal*, Vol. 9, 1971, pp. 1441-1446.
- <sup>3</sup>Benenson, D.M. and Cenker, A.A., Jr., "Effects of Velocity and Current on Temperature Distribution within Cross-Flow (Blown) Electric Arcs," *Transactions of the ASME, Journal of Heat Transfer*, Vol. 92, Ser. C, 1970, pp. 276-284.
- <sup>4</sup>Maldonado, C.D. and Olsen, H.N., "New Method for Obtaining Emission Coefficients from Emitted Spectral Intensities. Pt. II—Asymmetrical Sources," *Journal of the Optical Society of America*, Vol. 56, 1966, pp. 1305-1313.
- <sup>5</sup>Winograd, Y.Y. and Klein, J.F., "Electric Arc Stabilization in Crossed Convective and Magnetic Fields," *AIAA Journal*, Vol. 7, 1969, pp. 1699-1706.
- <sup>6</sup>Bond, C.E., "Slanting of a Magnetically Stabilized Electric Arc in Transverse Supersonic Flow," *Physics of Fluids*, Vol. 9, 1965, pp. 705-710.
- <sup>7</sup>Nicolai, L.M. and Kuethe, A.M., "Properties of Magnetically Balanced Arcs," *Physics of Fluids*, Vol. 12, 1969, pp. 2072-2083.
- <sup>8</sup>Malghan, V.R. and Benenson, D.M., "Analysis of Cross-Flow Arcs in Transverse Magnetic Fields," *IEEE Transactions on Plasma Sciences*, Vol. PS-1, 1973, pp. 38-46.

## Laser Schlieren for Study of Solid-Propellant Deflagration

James R. Andrews\* and David W. Netzer†  
Naval Postgraduate School, Monterey, Calif.

### Introduction

THE major objective of this study was to develop a laser schlieren (optically active aperture) system designed to eliminate the problem of self-luminous interference during flowfield studies and to apply it to the study of ammonium perchlorate deflagration. Developments in laser light source optical systems, including schlieren, have been reported by Lu<sup>1</sup> and Oppenheim.<sup>2</sup> These systems are potentially valuable tools for propellant combustion studies.

A major problem in observing surface behavior and the gas phase just above the surface during high-pressure combustion of certain propellants is the visible light or self-luminous interference effects from the combustion zone. As the pressure is raised, the combustion zone tends to move closer to the

Received Nov. 10, 1975; revision received Dec. 15, 1975. This work was sponsored by Naval Sea Systems Command, Contract ORD 331-007/551-1-332-303.

Index categories: Combustion in Gases; Combustion in Heterogeneous Media; Fuels and Propellants, Properties of.

\*Lieutenant Commander, U.S. Navy.

†Associate Professor, Department of Aeronautics. Member AIAA.